

## Ferromagnetism in iron-chromium alloys. I. Bulk magnetization measurements\*

A. T. Aldred

*Argonne National Laboratory, Argonne, Illinois 60439*

(Received 19 January 1976)

Bulk magnetization measurements were made between 5 and 300 K in fields up to 14 kOe on a series of iron-chromium alloys containing from 2- to 70-at.% Cr. The temperature dependence of the magnetization was analyzed to yield spin-wave stiffness coefficients that are systematically different from values obtained directly by inelastic-neutron-scattering measurements. The concentration dependence of the mean moment is approximately linear and is close to the Slater-Pauling curve. However, subtle deviations from linearity reflect the concentration dependence of the individual iron and chromium moments, which is presented in part II. The concentration dependence of the moments can be approximately reproduced by existing coherent-potential-approximation calculations.

### I. INTRODUCTION

The number of iron-base body-centered-cubic (bcc) solid-solution alloy systems in which the concentration dependence of the mean magnetic moment, as determined by magnetization measurements, can be studied over a wide range of concentration is quite limited. Only the iron-vanadium<sup>1</sup> and iron-chromium<sup>1,2</sup> systems have critical concentrations at which the ferromagnetism disappears as a function of concentration in the solid-solution region.

In iron-vanadium alloys, apart from the dilute region (0–2-at.% V) and the critical region (60–72-at.% V), the mean magnetic moment appears to decrease linearly with an increase in vanadium concentration. This rate of decrease is consistent with the Slater-Pauling<sup>3</sup> rigid-band analysis of magnetic moments in 3*d* transition-metal alloys. The rather sparse data for iron-chromium alloys<sup>1,2</sup> show an initial decrease of moment in iron-rich alloys that is consistent with the Slater-Pauling curve, but at higher chromium concentrations the data are rather uncertain. Shull and Wilkinson<sup>4</sup> have performed magnetic elastic-neutron-scattering experiments on iron-chromium alloys containing 15-, 29-, and 46-at.% Cr. The results yield the difference in average moment on the two species, and when combined with the mean magnetic moments obtained from magnetization measurements, give the average moments associated with both the iron and chromium atoms. These moments show a considerable nonlinear concentration dependence, and, strikingly, the average chromium moment appears to change sign near 40-at.% Cr.

In the present work, the mean-magnetic-moment values for iron-chromium alloys have been determined in detail as a function of concentration by means of bulk magnetization measurements. The

temperature dependence of the magnetization has been analyzed in terms of spin-wave theory to yield spin-wave stiffness coefficients, which are compared with those obtained directly by inelastic-neutron-scattering experiments.<sup>5</sup> Alloys that contain 70–80-at.% Cr, with Curie temperatures below room temperature, show complicated magnetic behavior. Although they appear to undergo bulk transitions to the ferromagnetic state on cooling, the field dependence of the magnetization is quite large and cannot be attributed to magnetocrystalline anisotropy inasmuch as the anisotropy fields in this composition range are small<sup>6</sup> (<100 Oe). The magnetic properties of alloys in the composition range 70–85-at.% Cr will be considered in a separate publication.

The phase diagram of the iron-chromium system<sup>7</sup> is simple at high temperatures, and apart from the  $\gamma$  loop, a complete range of bcc solid solutions exists from 820°C to the solidus. Alloys quenched from this solid-solution region to room temperature retain their bcc structure, but evidence from diffuse-neutron-scattering measurements<sup>8</sup> shows the presence of short-range clustering (characteristic of the high-temperature solid solution) in alloys quenched from above 820°C. The presence of clustering is consistent with the miscibility gap that occurs in this system at lower temperatures (<520°C).<sup>7</sup>

### II. EXPERIMENTAL AND DATA ANALYSIS

The alloys and samples were prepared, with the starting materials 99.99 wt% pure, by techniques described previously.<sup>9</sup> Arc-melted buttons were given homogenization heat treatments for one week at 1150°C followed by one week at 825°C and then were water quenched. Selected alloys were analyzed, and the close agreement between analyzed and nominal compositions was consistent with the negligible weight losses on melting. There-

fore, the nominal compositions were taken as correct for all alloys investigated. The concentration dependence of the lattice parameters and the densities determined for each of the alloys also indicate that the nominal compositions are correct.

Specific magnetizations  $\sigma_{H,T}$  (emu/g) were measured by a standard force technique.<sup>9,10</sup> Magnetic isotherms were obtained between 5 and 295 K over an applied field range of 0 to 14 kOe at intervals of 1 kOe. The applied fields were corrected for the demagnetizing field of the specimen ( $\leq 4$  kOe) to yield the internal field  $H_i$ . Magnetic field gradients were calibrated with a single-crystal nickel sample for which a magnetization of 58.57 emu/g at 5 K was assumed.<sup>11</sup>

The temperature dependence of the magnetization of each alloy was analyzed in terms of spin-wave theory. In the limit of a quadratic dispersion law, the expression for the specific magnetization  $\sigma_{H,T}$  as a function of field  $H$  and temperature  $T$  is<sup>12,13</sup>

$$\sigma_{H,T} = \sigma_{0,0} - \frac{g\mu_B}{\rho} \left( \frac{kT}{4\pi D} \right)^{3/2} F\left(\frac{3}{2}, t\right), \quad (1)$$

where  $g$  is the Landé splitting factor,  $\mu_B$  is the Bohr magneton,  $\rho$  is the density,  $k$  is Boltzmann's constant,  $D$  is the spin-wave stiffness coefficient, and  $F\left(\frac{3}{2}, t\right)$  is the Bose-Einstein integral function,

$$F\left(\frac{3}{2}, t\right) = \sum_{n=1}^{\infty} n^{-3/2} e^{-n/t}, \quad (2)$$

where  $t$  is  $kT/g\mu_B H$ . The field  $H$  is the sum of the internal field and the anisotropy field. It was shown in a previous paper<sup>14</sup> that Eq. (1) provides a good representation of the temperature dependence of the magnetization of pure iron if it is modified to include a temperature-dependent  $D$  of the form

$$D = D_0 - D_1 T^2. \quad (3)$$

In this way, the variation of  $D$  with temperature

was found to be in quantitative agreement with that obtained by Stringfellow<sup>15</sup> from neutron scattering studies. All samples used in the present work are polycrystalline in nature, and the contributions to Eq. (1) that arise from the "approach-to-saturation" terms were also considered in Ref. 14. In addition to a possible term of unknown magnitude varying as  $H^{-1}$  and related to the presence of defects in the sample, a contribution going as  $H^{-2}$  should be present with a coefficient proportional to the square of the first anisotropy constant  $K_1(T)$ , where

$$K_1(T)/K_1(0) \propto (\sigma_{0,T}/\sigma_{0,0})^n. \quad (4)$$

Thus it is possible to analyze the temperature and field dependence of a polycrystalline material in terms of Eq. (1), modified in terms of Eqs. (3) and (4), by least-squares fitting with  $\sigma_{0,0}$ ,  $D_0$ ,  $D_1$ ,  $K_1(0)$ , and  $n$  treated as disposable parameters. For a number of alloys investigated, particularly at higher chromium concentrations, an improved match to the data was obtained with the inclusion of an  $H^{-1}$  term with coefficient  $a$ , i.e., a six-parameter fit. For the 65-at.% Cr alloy, it was possible to account for the "approach-to-saturation" field dependence with only a temperature-independent  $H^{-1}$  term, i.e., a four-parameter fit, whereas for 70-at.% Cr, a similar analysis was used with an additional linear  $H$  (susceptibility) term included (five-parameter fit). The details of the various parameters used in the different fits (labeled *A*, *B*, *C*, and *D*) are given in Table I. In the analysis, a value of the Landé splitting factor varying linearly from 2.09 in pure iron<sup>16</sup> to 2.07 at 70-at.% Cr (Ref. 6) was used, together with density values measured for each specimen. The anisotropy field was calculated for each composition from an interpolation of the anisotropy-constant data of David and Heath<sup>6</sup> and Hall.<sup>17</sup> A discussion of the magnitude and sources of experimental error is given in Ref. 14.

TABLE I. Parameters used in spin-wave analysis of the temperature dependence of the magnetization of Fe-Cr alloys.

Identification of fit	Number of parameters	Parameters used <sup>a</sup>
<i>A</i>	5	$\sigma_{0,0}$ , $D_0$ , $D_1$ , $K_1(0)$ , $n$
<i>B</i>	6	$\sigma_{0,0}$ , $D_0$ , $D_1$ , $K_1(0)$ , $n$ , $a$
<i>C</i>	4	$\sigma_{0,0}$ , $D_0$ , $D_1$ , $a$
<i>D</i>	5	$\sigma_{0,0}$ , $D_0$ , $D_1$ , $a$ , $\chi$

<sup>a</sup>  $\sigma_{0,0}$ , spontaneous magnetization at 0 K;  $D_0$ , spin-wave stiffness coefficient at 0 K;  $D_1$ , temperature coefficient of stiffness constant;  $K_1(0)$ , first anisotropy constant;  $n$ , exponent of anisotropy constant;  $a$ , coefficient of  $H^{-1}$  term;  $\chi$ , susceptibility term (linear in  $H$ ).

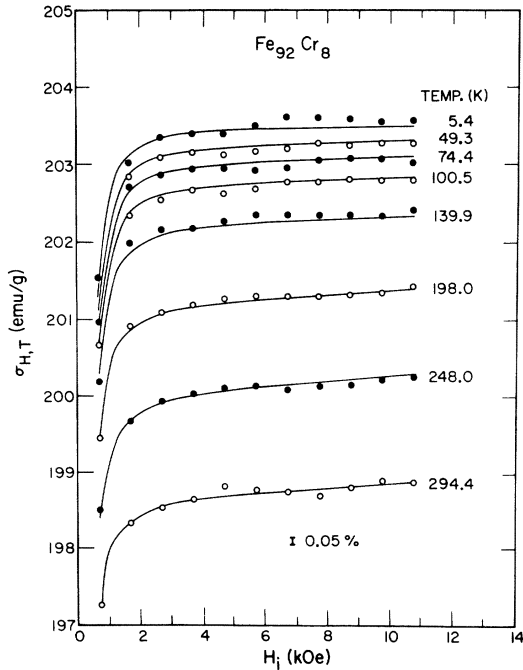


FIG. 1. Field dependence of the magnetization of an Fe-Cr alloy containing 8-at.% Cr at various temperatures. The lines represent a fit to the modified spin-wave equation (see text).

### III. RESULTS

To illustrate the general magnetic behavior of Fe-Cr alloys, some typical experimental data will be presented. The magnetic isotherms for the alloy containing 8-at.% Cr are shown in Fig. 1. The magnetization decreases by  $\sim 2\%$  between 5 and 295 K; this is similar to the change in pure iron, and the Curie temperature  $T_F$  at this composition<sup>18</sup> is quite close to that of iron. The solid lines represent a fit to the modified version of Eq. (1) with 5 parameters and 88 data points (fit A, Table I); it is evident that the spin-wave equation provides a good representation of the data. The rapid decrease in the anisotropy ( $H^{-2}$ ) term with an increase in temperature is apparent in the low-field data. To show the temperature dependence of the magnetization more clearly, the data at  $H_i = 8.7$  kOe have been replotted in Fig. 2 as a function of  $T^{3/2} F(\frac{3}{2}, T)$ . The dashed line represents a fit to the data with a temperature-independent  $D$ , i.e., a four-parameter version of fit A with the  $D_1$  parameter removed, and the solid line is the five-parameter fit discussed above. The curvature arising from a temperature-dependent  $D$  is similar in magnitude to that in iron.<sup>14</sup>

The magnetic isotherms determined for the 30-at.% Cr alloy are shown in Fig. 3; the relative temperature dependence up to room temperature is

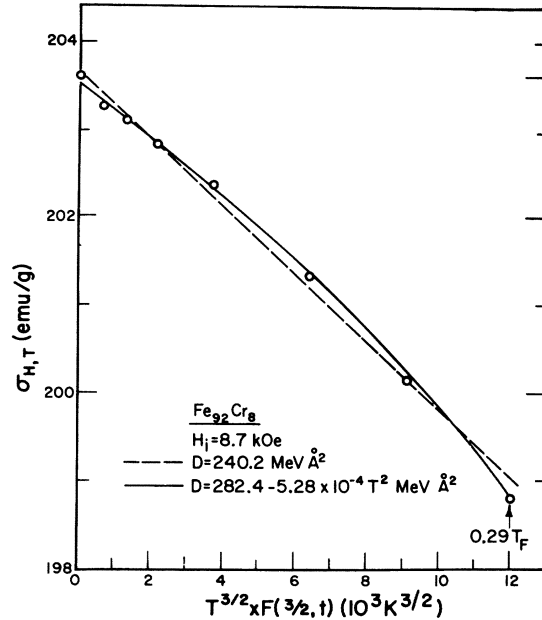


FIG. 2. Magnetization data from Fig. 1 at  $H_i = 8.7$  kOe plotted as a function of  $T^{3/2}$ . The solid line represents the same fit as in Fig. 1; the dashed line represents a simplified fit as noted in the text.

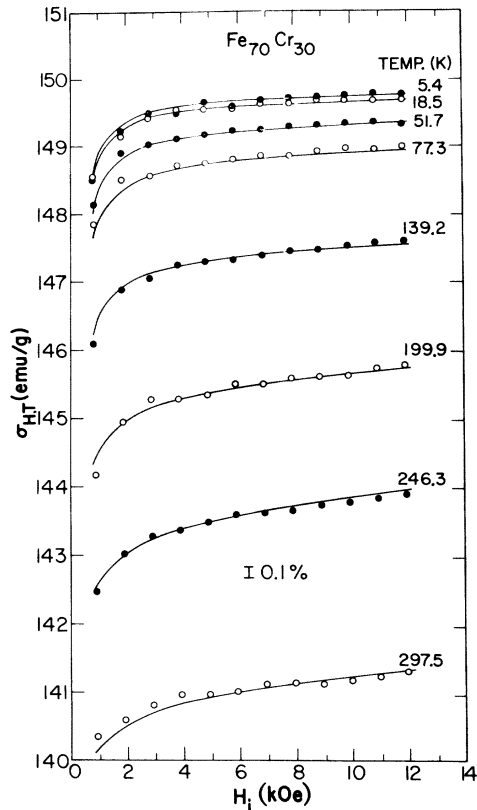


FIG. 3. Field dependence of the magnetization of an Fe-Cr alloy containing 30-at.% Cr at various temperatures. The lines represent a fit to the modified spin-wave equation (see text).

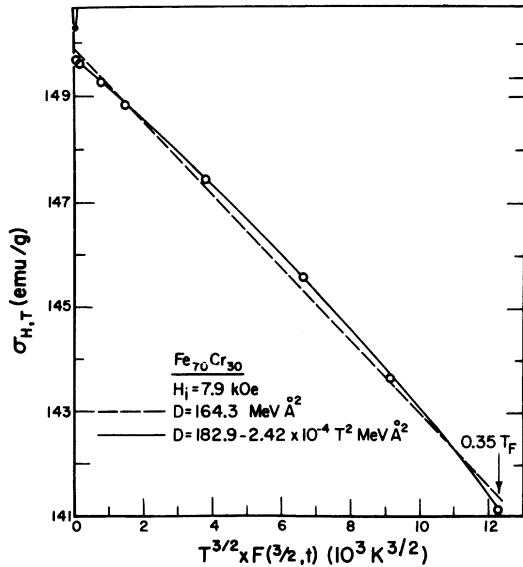


FIG. 4. Magnetization data from Fig. 3 at  $H_i = 7.9$  kOe plotted as a function of  $T^{3/2}$ . The solid line represents the same fit as in Fig. 3; other details as in Fig. 2.

much greater ( $\sim 6\%$ ) than for the 8-at.% Cr alloy. Figure 3 also illustrates the decrease in the  $H^{-2}$  term (low-field data) as the temperature increases, and the increase in the spin-wave contribution to the field dependence at high temperatures and high fields for the 30-at.% Cr alloy as compared with the 8-at.% Cr alloy (Fig. 1). The solid lines represent a six-parameter least-squares fit to 96 data points (fit B). The temperature dependence of the magnetization for the 30-at.% Cr sample at 7.9 kOe is shown in Fig. 4 together with the results of the fit. Although the data were obtained over a larger relative range of temperature ( $\leq 0.35T_F$ ), the curvature of the  $T^{3/2}$  plot is less than in the case of the 8-at.% Cr alloy, and thus the value of  $D_i$  [Eq. (3)] has decreased more than the corresponding value of  $D_0$ .

The magnetic isotherms for the 50-at.% Cr alloy are plotted in Fig. 5. The magnetization decreases by  $\sim 18\%$  between 5 K and room temperature ( $\sim 0.49T_F$ ). The small approach-to-saturation term and the large contribution from the spin-wave term to the field dependence at high temperatures (approximately linear in  $H$  over this field range) is again evident. The solid lines represent the same six-parameter fit as used for the 30-at.% Cr alloy (fit B). The temperature dependence of the magnetization at  $H_i = 7.5$  kOe for the 50-at.% Cr alloy is shown in Fig. 6. The small curvature in the  $T^{3/2}$  plot necessitated more closely spaced (as a function of temperature) data points (total of 204) to determine the temperature dependence of  $D$  with reasonable precision. The spin-wave equa-

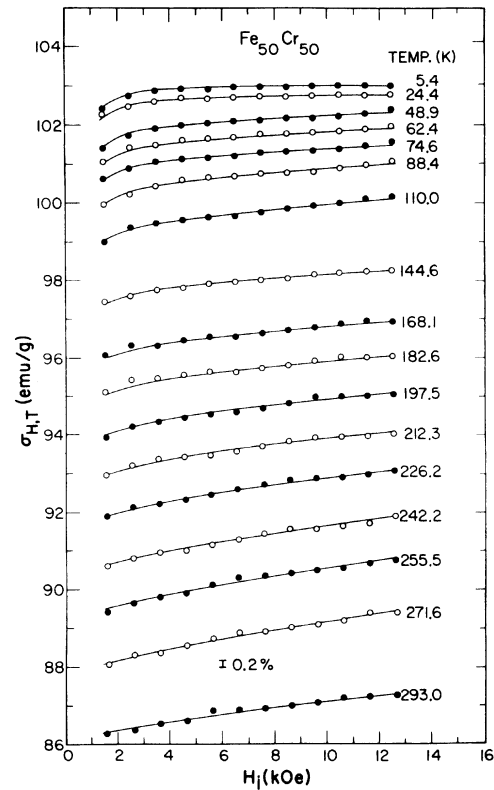


FIG. 5. Field dependence of the magnetization of an Fe-Cr alloy containing 50-at.% Cr at various temperatures. The lines represent a fit to the modified spin-wave equation (see text).

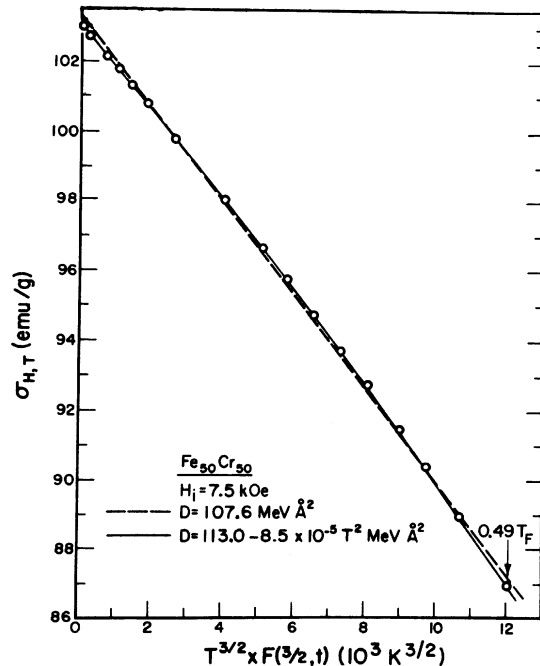


FIG. 6. Magnetization data from Fig. 5 at  $H_i = 7.5$  kOe plotted as a function of  $T^{3/2}$ . The solid line represents the same fit as in Fig. 5; other details as in Fig. 2.

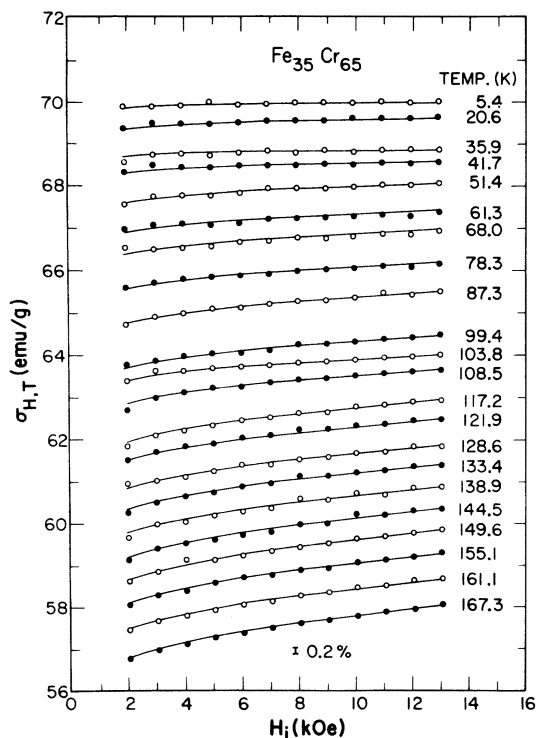


FIG. 7. Field dependence of the magnetization of an Fe-Cr alloy containing 65-at.% Cr at various temperatures. The lines represent a fit to the modified spin-wave equation (see text).

tion gives a good fit to the data up to  $\sim 0.5T_F$ .

The decrease in Curie temperature with an increase in chromium concentration is such that, for alloys containing more than 50-at.% Cr, the maximum temperature of the measurement is greater than  $0.5T_F$ . It was found, for these alloys, that the spin-wave fit only gave a good representation of the data up to  $\sim 0.5T_F$ . As an example, the magnetization data up to 170 K for the 65-at.% Cr alloy are shown in Fig. 7. The solid lines again represent the spin-wave fit, although, in this case, the experimental field dependence can be accounted for almost completely by the spin-wave term, and it was necessary to include only a temperature-independent  $H^{-1}$  term to Eq. (1), i.e., a four-parameter fit (fit C). The temperature dependence of the magnetization of the 65-at.% Cr alloy at 10.0 kOe is given in Fig. 8. Because of the restricted absolute temperature range of the data, the horizontal scale is considerably expanded with respect to Figs. 2, 4, and 6. The deviations from a  $T^{3/2}$  dependence are quite small, but a real change in sign of the curvature is apparent; i.e., the fitted value of the coefficient  $D_1$  in Eq. (3) changes sign. A similar effect is observed in the data for the 60- and 70-at.% Cr alloys (not shown).

To reproduce the field and temperature dependence of the magnetization of the 70-at.% Cr alloy, it was necessary to include a temperature-independent linear susceptibility term in the analysis (fit D).

#### IV. DISCUSSION

The results of the least-squares analysis of the magnetization data for each alloy are given in Table II, which also includes the field and temperature range of the analysis and the value of the mean magnetic moment per atom  $\bar{\mu}$  calculated from the fitted value of the spontaneous magnetization  $\sigma_{0,0}$ . The anisotropy constants determined in the analysis are consistent with the values obtained directly by David and Heath<sup>6</sup> and Hall.<sup>17</sup> The concentration dependence of the spin-wave stiffness coefficient  $D_0$  is shown in the lower portion of Fig. 9; results of Lowde *et al.*,<sup>5</sup> obtained directly by means of inelastic-neutron-scattering techniques, are also included. The value given by Lowde *et al.* for pure iron plotted in Fig. 9 is  $\sim 10\%$  lower than a more recent value given by the same group<sup>15</sup>; it was shown in Ref. 14 that the more recent value is in agreement with the value of  $D_0$  obtained from an analysis of magnetization data. Thus it is probably appropriate to increase all the neutron values in Fig. 9 by  $\sim 10\%$ , and this would, of course, increase the discrepancy between the two sets of values. The fitting errors (Table II) and probable data errors (Ref. 14) are too small to account for this discrepancy. The

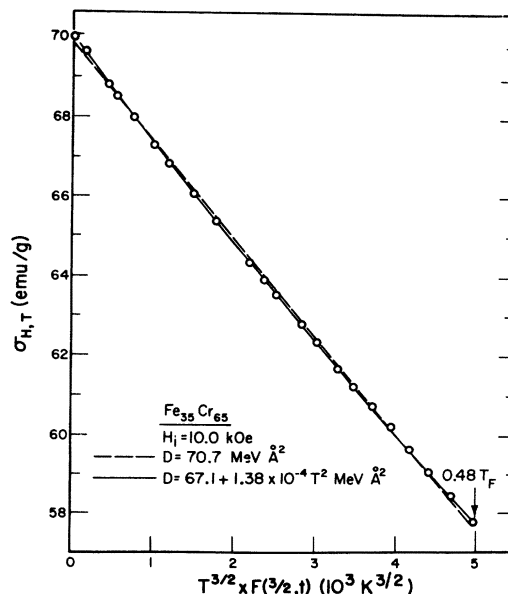


FIG. 8. Magnetization data from Fig. 7 at  $H_i = 10.0$  kOe plotted as a function of  $T^{3/2}$ . The solid line represents the same fit as in Fig. 7; other details as in Fig. 2.

TABLE II. Results of least-squares fits of magnetization data for Fe-Cr alloy to a modified spin-wave equation. Details of the different fits are given in Table I and the text.<sup>a</sup>

Alloy concn. (at.% Cr)	Fit used	$\sigma_{0,0}$ (emu/g)	$D_0$ (meVÅ <sup>2</sup> )	$D_1$ (10 <sup>-4</sup> meVÅ <sup>2</sup> K <sup>-2</sup> )	$K_1(0)$ (10 <sup>5</sup> erg/cm <sup>3</sup> )	$n$	$a$ (Oe emu/g)	rms error (emu/g)	Internal field range (kOe)	Max. $T/T_F$	$\bar{\mu}$ ( $\mu_B$ /atom)
2.0	A	217.72(1)	301(3)	5.12(37)	4.40(14)	25(4)	...	0.041	1.4-10.4	0.28	2.174
4.0	A	212.72(2)	297(5)	4.59(54)	4.88(7)	11(2)	...	0.051	0.7-10.7	0.28	2.121
6.0	A	208.33(2)	296(6)	5.54(64)	4.27(5)	9(1)	...	0.059	0.5-10.5	0.28	2.074
8.0	A	203.50(2)	282(6)	5.28(63)	4.08(10)	8(2)	...	0.063	0.7-10.7	0.29	2.023
10.0	A	198.36(3)	266(4)	4.45(47)	4.14(4)	9(1)	...	0.055	0.5-10.5	0.29	1.969
12.0	B	193.24(2)	260(3)	4.59(30)	3.32(9)	6(1)	884(84)	0.050	0.5-10.4	0.30	1.916
15.0	A	185.69(2)	249(3)	3.98(40)	3.55(11)	15(2)	...	0.058	0.8-10.8	0.30	1.837
20.0	A	173.34(1)	227(2)	3.88(19)	3.75(17)	14(3)	...	0.043	1.5-11.5	0.31	1.709
25.0	B	161.38(3)	189(1)	1.61(16)	3.25(45)	10(3)	537(196)	0.041	1.2-11.4	0.33	1.586
30.0	B	149.81(3)	183(1)	2.42(16)	1.54(54)	18(13)	751(172)	0.054	0.8-12.0	0.35	1.467
35.0	B	138.05(3)	163(1)	1.90(16)	1.80(52)	20(11)	555(197)	0.049	1.0-12.2	0.37	1.347
40.0	B	126.52(4)	147(1)	1.24(10)	2.04(77)	13(9)	915(278)	0.049	1.2-12.4	0.39	1.230
45.0	B	115.03(3)	128(1)	1.03(7)	1.60(69)	6(6)	526(223)	0.050	1.1-12.4	0.44	1.114
50.0	B	103.06(2)	113(1)	0.85(3)	2.40(35)	6(2)	204(159)	0.043	1.3-12.6	0.49	0.995
55.0	B	92.56(3)	97.9(5)	0.43(7)	1.30(21)	3(1)	1089(146)	0.056	0.5-12.7	0.48	0.890
60.0	B	81.52(2)	83.1(3)	-0.12(6)	1.12(18)	6(2)	682(108)	0.051	0.6-12.8	0.49	0.781
65.0	C	70.05(1)	67.1(2)	-1.38(6)	...	...	273(49)	0.036	1.9-13.1	0.48	0.669
70.0	D <sup>b</sup>	57.58(5)	45.7(1)	-5.46(11)	...	...	418(142)	0.041	2.1-13.3	0.46	0.548

<sup>a</sup> Numbers in parentheses represent statistical uncertainties in final significant figure(s) of parameters.

<sup>b</sup> The fit includes a susceptibility term  $\chi = (1.46 \pm 0.36) \times 10^{-5}$  emu/g.

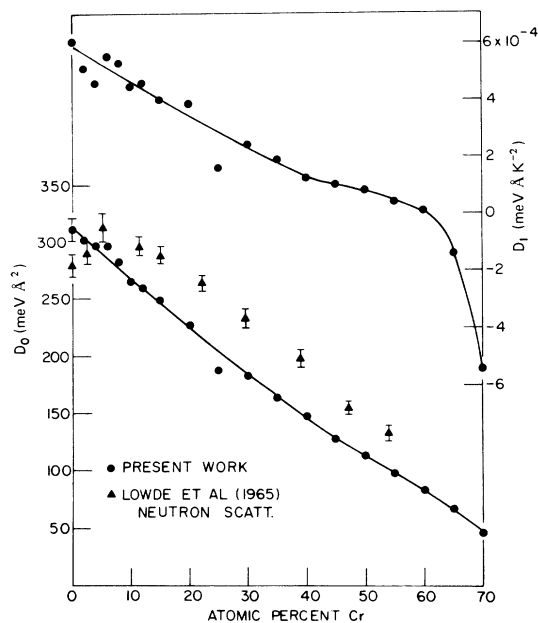


FIG. 9. Concentration dependence of the spin-wave stiffness constants for Fe-Cr alloys.

maximum in the neutron value of  $D_0$  near 5-at.% Cr is paralleled by a maximum in the Curie temperature<sup>18</sup>; however, the relative increase in  $T_F$  from pure iron is only  $\sim 1\%$  compared with the  $\sim 10\%$  effect in the neutron  $D_0$  value. Only a qualitative correlation between  $T_F$  and  $D_0$  was found in Fe-V alloys.<sup>5,19</sup>

The present  $D_0$  values show an essentially monotonic decrease with an increase in chromium concentration and extrapolate to zero close to the critical concentration of  $\sim 85$ -at.% Cr.<sup>1</sup> In view of the quantitative correlation between  $D_0$  values obtained by both neutron diffraction and magnetization techniques for Fe-V alloys,<sup>5,19</sup> it seems likely that the lack of correlation in Fe-Cr alloys indicates the presence of another contribution to the temperature dependence of the magnetization. Thompson *et al.*<sup>20</sup> have shown that, in general, a term should be present in the temperature dependence of the magnetization which arises from single-particle Stoner excitations and varies either as  $T^2$  or exponentially in  $T$ . A detailed comparison of the experimental temperature dependence of the magnetization of nickel with that calculated from neutron-diffraction-derived temperature-dependent stiffness constants has shown the presence of a single-particle contribution equal in magnitude to the spin-wave term.<sup>21</sup> Because the two powers of temperature are similar, an attempt to separate the single-particle temperature dependence from the spin-wave contribution simply by including an extra term in the least-squares

fit is not practicable, given the error limits of the present data. If the temperature dependence of the stiffness constant were independently available, the single-particle contribution could, of course, also be calculated by difference. Until such experimental information becomes available, or it is possible to obtain magnetization results with an order-of-magnitude greater precision, this situation cannot be resolved.

The concentration dependence of the second spin-wave coefficient  $D_1$  obtained in the present analysis is shown in the upper portion of Fig. 9. In light of the discussion above, the absolute values of  $D_1$  are open to question; however, the general trends should be valid. The monotonic decrease with an increase in chromium concentration is similar to that of  $D_0$ . The relative change is, however, more rapid, and  $D_1$  appears to go to zero close to 60-at.% Cr and change sign at higher concentrations; i.e., the curvature of the  $T^{3/2}$  plots changes sign (e.g., see Fig. 8). Stringfellow<sup>15</sup> has considered the temperature dependence of the spin-wave stiffness coefficient in iron (renormalization) and concludes that two terms are present, so that  $D_1$  [Eq. (3)] is the composite of one contribution going as  $T^2$  and one varying as  $T^{5/2}$ . It thus seems likely that the concentration dependence of the two terms in Fe-Cr alloys is sufficiently different to give a net sum (represented by  $D_1$ ) that changes sign as a function of concentration. Alternatively, the

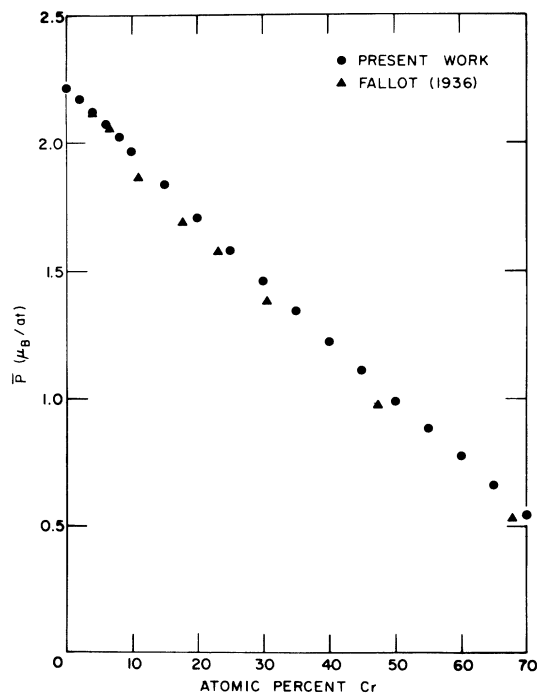


FIG. 10. Concentration dependence of the bulk magnetic moment for Fe-Cr alloys.

change in curvature of the  $T^{3/2}$  plots could indicate a breakdown of the spin-wave equation in fitting the data in this composition region. This is consistent with the fact noted earlier that the magnetism appears to be more inhomogeneous in this critical concentration region where ferromagnetism disappears.<sup>22-24</sup>

The concentration dependence of the mean magnetic moment is shown in Fig. 10; the earlier results of Fallot<sup>2</sup> are also plotted. The two sets of data are in excellent agreement at low chromium concentrations, but elsewhere Fallot's results fall consistently below the present ones. This deviation is most likely attributable to sample-preparation techniques. After induction melting his samples, Fallot annealed them for 2 h at 1050°C in vacuum and then slowly cooled them to 300°C over a period of 150 h before quenching to room temperature. In light of the present phase diagram,<sup>7</sup> the slow-cooling procedure is likely to have caused separation of the samples into iron-rich and chromium-rich phases. It is difficult, therefore, to consider Fallot's results as characteristic of homogeneous samples.

Although the present mean-moment data have an approximately linear concentration dependence, closer examination shows a much more subtle variation with composition, and a fifth-order polynomial is necessary to reproduce the data within the experimental error ( $\sim \pm 0.002\mu_B/\text{atom}$ ). The initial slope (as the chromium concentration tends to zero) given by this polynomial ( $\sim -2.1\mu_B/\text{atom}$ ) is close to that expected on the basis of a simple Slater-Pauling rigid-band analysis ( $-2.0\mu_B/\text{atom}$ ); the overall concentration dependence, however, yields an average slope of approximately  $-2.4\mu_B/\text{atom}$ .

Attempts have been made<sup>25</sup> to deduce rigid-band schemes for the Fe-Cr system that are consistent with the Slater-Pauling curve and the concentration dependence of the linear coefficient of the low-temperature specific heat<sup>26</sup> (which should be a measure of the density of states). However, a

band model yields no information about the location of the magnetic moments, and neutron diffraction results<sup>4,8</sup> indicate that the magnitude of the moments at the iron and chromium sites are quite different. A more appropriate model is the coherent-potential approximation<sup>27,28</sup> which has, as a starting point, the calculated density of states of pure iron.<sup>29,30</sup> With a suitable choice of parameters, such a scheme yields mean magnetic moments in good agreement with Fallot's earlier results<sup>2</sup> and approximately reproduces the neutron-determined iron and chromium moments.<sup>4,8</sup> The present mean moments, inasmuch as they are more precisely determined than Fallot's data, should provide much stronger constraints on the coherent-potential approximation. It is interesting that the complicated concentration dependence of the individual iron and chromium moments yields an almost linear concentration dependence of the mean moment. The subtle deviations from linearity of the present mean-moment data presumably reflect details of the concentration dependence of the individual moments.

In summary, detailed magnetization measurements have been made, as a function of temperature, field, and composition, on a series of bcc Fe-Cr alloys. The temperature dependence of the magnetization has been analyzed in terms of spin-wave theory. The bulk magnetic moment, as determined from the spontaneous magnetization at 0 K, has been found to have a concentration dependence with subtle variations from the linear behavior predicted from the Slater-Pauling curve. Details of the individual magnetic moments at the iron and chromium sites will be presented in Paper II.

#### ACKNOWLEDGMENTS

The author would like to thank P. H. Froehle for experimental and computational assistance, and Dr. J. S. Kouvel, Dr. G. H. Lander, and Dr. T. J. Hicks for helpful discussions.

\*Work supported by the U. S. Energy Research and Development Administration.

<sup>1</sup>M. V. Nevitt and A. T. Aldred, *J. Appl. Phys.* **34**, 463 (1963).

<sup>2</sup>M. Fallot, *Ann. Phys. (Paris)* **6**, 305 (1936).

<sup>3</sup>J. C. Slater, *J. Appl. Phys.* **8**, 385 (1937); L. Pauling, *Phys. Rev.* **54**, 899 (1938).

<sup>4</sup>C. G. Shull and M. K. Wilkinson, *Phys. Rev.* **97**, 304 (1955).

<sup>5</sup>R. D. Lowde, M. Shimizu, M. W. Stringfellow, and B. H. Torrie, *Phys. Rev. Lett.* **14**, 698 (1965).

<sup>6</sup>P. David and M. Heath, *J. Phys. (Paris)* **32**, C1-112

(1971).

<sup>7</sup>R. P. Elliott, *Constitution of Binary Alloys, First Supplement* (McGraw-Hill, New York, 1965).

<sup>8</sup>A. T. Aldred, B. D. Rainford, J. S. Kouvel, and T. J. Hicks, following paper, *Phys. Rev. B* **14**, 228 (1976).

<sup>9</sup>A. T. Aldred, *J. Appl. Phys.* **37**, 671 (1966).

<sup>10</sup>A. T. Aldred, *J. Phys. C* **1**, 244 (1966).

<sup>11</sup>H. Danan, A. Herr, and A. J. P. Meyer, *J. Appl. Phys.* **39**, 669 (1968).

<sup>12</sup>F. Keffer, *Handb. Phys.* **18**, 21 (1966).

<sup>13</sup>T. F. Smith, W. E. Gardner, and J. I. Budnick, *Phys. Lett. A* **27**, 326 (1968).



- <sup>14</sup>A. T. Aldred and P. H. Froehle, *Int. J. Magn.* 2, 195 (1972).
- <sup>15</sup>M. W. Stringfellow, *J. Phys. C* 1, 950 (1968).
- <sup>16</sup>A. J. P. Meyer and G. Asch, *J. Appl. Phys.* 32, 330 (1961).
- <sup>17</sup>R. C. Hall, *J. Appl. Phys.* 31, 1037 (1960).
- <sup>18</sup>F. Adcock, *J. Iron Steel Inst. (London)* 124, 99 (1931).
- <sup>19</sup>A. T. Aldred, *Int. J. Magn.* 2, 223 (1972).
- <sup>20</sup>E. D. Thompson, E. P. Wohlfarth, and A. C. Bryan, *Proc. Phys. Soc. Lond.* 83, 59 (1964).
- <sup>21</sup>A. T. Aldred, *Phys. Rev. B* 11, 2597 (1975).
- <sup>22</sup>Y. Ishikawa, R. Tournier, and J. Filippi, *J. Phys. Chem. Solids* 26, 1727 (1965).
- <sup>23</sup>R. D. Shull and P. A. Beck, *AIP Conf. Proc.* 24, 95 (1975).
- <sup>24</sup>B. Loegel, *J. Phys. F* 5, 497 (1975).
- <sup>25</sup>L. Berger, *Phys. Rev.* 137, A220 (1965).
- <sup>26</sup>C. H. Cheng, C. T. Wei, and P. A. Beck, *Phys. Rev.* 120, 426 (1960).
- <sup>27</sup>H. Hasegawa and J. Kanemori, *J. Phys. Soc. Jpn.* 33, 1607 (1972).
- <sup>28</sup>G. Frollani, F. Menzinger, and F. Sacchetti, *Phys. Rev. B* 11, 2030 (1975).
- <sup>29</sup>S. Wakoh and J. Yamashita, *J. Phys. Soc. Jpn.* 21, 1712 (1966).
- <sup>30</sup>K. J. Duff and T. P. Das, *Phys. Rev. B* 3, 192 (1971).